7-2012

Production and Characterization of Biodegradable Nanofibers via Forcespinning™ Technology

Zachary T. McEachin
University of Texas-Pan American

PRODUCTION AND CHARACTERIZATION OF BIODEGRADABLE NANOFIBERS VIA FORCESPINNING™ TECHNOLOGY

A Thesis
by
ZACHARY T. MCEACHIN

Submitted to the Graduate School of
The University of Texas-Pan American
In partial fulfillment of the requirements for the degree of

MASTER OF SCIENCE

July 2012

Major Subject: Mechanical Engineering

PRODUCTION AND CHARACTERIZATION OF BIODEGRADBLE NANOFIBERS VIA FORCESPINNING™ TECHNOLOGY

A Thesis
by
ZACHARY T. MCEACHIN

COMMITTEE MEMBERS

Dr. Karen Lozano
Chair of Committee

Dr. Dorina Mihut
Committee Member

Dr. Jose Gutierrez
Committee Member

July 2012

ABSTRACT

McEachin, Zachary T., Production and Characterization of Biodegradable Nanofibers via Forcespinning™ Technology. Master of Science (MS), July, 2012, 41 pp., 4 tables, 22 figures, references, 41 titles.

Among the myriad of methods for polymer nanofiber production, there are only a few methods that can produce submicron range fibers in bulk from melt or solution samples. The Forcespinning™ method allows a substantial increase in sample yield; this greatly reduces the time needed to produce bulk quantities of fibers which may be critical in many fields of research and industry, in particularly in fields relating to biopolymers. The aim of the first study was to utilize this method to form non-woven mats of polycaprolactone (PCL) nanofibers and to quantitatively analyze the production and characterization of the produced fibers. The morphology and degree of crystallinity were characterized by SEM, DSC, and XRD. Additionally, as a second project, microcrystalline cellulose fibers were successfully regenerated from the ionic liquid 1-ethyl-3-methylimidazolium acetate using the Forcespinning™ method. Similarly, the cellulose fibers were subjected to various characterization techniques such as SEM, XRD, TGA, and FITR.

DEDICATION

I would like to dedicate this thesis to my loving and always understanding parents Richard and Susan McEachin, whose love, continuous support, and motivation allowed me to become who I am today. Also, to my beautiful wife Valery McEachin and son Zachary Alexander McEachin, whom without I would be lost. Lastly, to my brothers and sister; Marilyn Hart, David Marshall and Mark Marshall

ACKNOWLEDGMENTS

I owe my deepest gratitude to Dr. Karen Lozano, chair of my thesis committee, whose encouragement, mentoring, and advice since the beginning of my graduate studies allowed me to complete my thesis. Additionally, I would like to thank my thesis committee members Dr. Jose Gutierrez and Dr. Dorina Mihut for their continuous support and motivation. Furthermore, I would like to acknowledge Dr. David Allen, Dr. Arturo Fuentes, Dr. Robert Jones, and Dr. Constantine Tarawneh for their always insightful yet often times unrelated discussions throughout the last two years. Lastly I would like to thank all of my fellow lab mates for their support, understanding, and most of all friendship. To all mentioned, I am truly indebted.

TABLE OF CONTENTS

Page

LIST OF TABLES

Page

LIST OF FIGURES

Page

CHAPTER I

INTRODUCTION

The production of fine polymer fibers has recently garnered much attention due to their potential applications. These nanofibrous polymers are unique due in part to their superior mechanical properties, large surface area to volume ratio, and their potential to resemble cellular topographies. Nonwoven polymer fibers in the nanometer range are currently being investigated for uses in filtration, composite reinforcements, chemical sensors, and tissue scaffolding [1], [2], [3], [4]. Despite the recent interest in non-woven nanofibers, significant challenges remain in their implementation due to the lack of high throughput production.

In the last few decades, electrospinning has been the most widely used [5],[6] and promising method of producing fine fibers [7]. Electrospinning utilizes high voltage electrostatic forces between an electrically charged polymer solution fed via a metering pump and a conductive collector in order to initiate fiber formation [8]. Although a simple and laboratory efficient method for fiber production, the electrospinning method poses many disadvantages including: 1) use of a high voltage power source (>10kV), 2) limited to solvents within a certain range of dielectric constant, and 3) low fiber yield [8], [9].

However, with the advent of Forcespinning™ technology, the obstacles commonly encountered with use of electrospinning are overcome. Forcespinning utilizes centrifugal forces in order to promote fiber elongation, therefore both conductive and nonconductive polymer solutions and polymer melts fiber can be spun without the need of electric fields [6], [10]. Also

the productivity of this method (1g/min using a 1-prong spinneret), at the lab scale, has considerable gains over laboratory scale electrospinning (0.3g/hr) [9]. The morphology of forcespun fibers is dependent on solution parameters and device configurations such as solution/melt viscosity, orifice diameter, and fiber collection methods.

In this thesis, Forcespinning™ technology was exploited to produce fine fibers of biodegradable polymers. The research presented herein is the accumulation of two projects conducted over the past two years. Project 1, titled *"Production and Characterization of Polycaprolactone via Forcespinning™ Technology"* utilizes polycaprolactone (PCL) dissolved in dichloromethane (DCM) to produces ultrafine fibers, while Project 2, titled *"High-Yield Production of cellulose micro/nano-fibers regenerated from the ionic liquids"* concerns the fabrication and characterization of underivatized cellulose fibers from the room temperature ionic liquid 1-ethyl-3-methylimidazolium acetate. Chapter 2 of this thesis is dedicated to project 1 (PCL/DCM system), while Chapter 3 is dedicated to project 2 (Cellulose/EMIM Ac). Furthermore, Chapter 4 (Conclusion) briefly summarizes the results from both projects. Lastly, Chapter 5 highlights future scientific research endeavors the author plans to pursue.

CHAPTER II

POLYCAPROLACTONE

2.1 Introduction

Polycaprolactone (PCL) is a biocompatible and bioresorbable semi-crystalline aliphatic polyester that has found uses in both industrial and biomedical applications [11]. The biodegradable nature of PCL can be attributed to the hydrolytic degradation of its ester bond and ultimately the non-toxic degradation metabolites that are formed and either secreted directly or metabolized in the Krebs cycle [12], [13], [14]. PCL as a homopolymer has a degradation time between two and four years, however the degradation time of PCL can be greatly varied when copolymerized with other biodegradable polymers [15]. Due to its biodegradability and exceptional mechanical properties [16], PCL fibers have found extensive uses as scaffolds or substrates for tissue engineering, drug delivery systems, and constituent materials in various nanocomposites [7], [17].

PCL has been used extensively as a scaffold for cell regeneration in a wide array of tissues. Choi et al. have successfully created a PCL/Collagen nanofibrous scaffold in order to facilitate muscle cell regeneration in large skeletal muscle defects. They showed that these nanofibrous meshes support cell adhesion and proliferation and when aligned can augment the formation of myotubes [18]. Similarly, PCL has also shown promising results as a synthetic bone scaffold. Porter et al. have studied PCL nanofibers as a replacement to the common bone graft material, autogenous cancellous bone. They found that the PCL nanofibers provided a

biomimetic environment in which there was an increase in both a short and long-term response of mesenchymal stem cells as well as a significant increase in the production of the noncollagenous extracellular matrix proteins, osteocalcin and osteopontin [19].

Akin to tissue engineering, PCL has been used in the research of novel drug delivery systems (DDS). Zamani et al. successfully encapsulated the antibiotic drug metronidazole benzoate (MET) in electrospun PCL nanofibers [20]. They concluded that the antibiotic was indeed released via diffusion through the PCL fibers, referring to this as Fickian diffusion. They also found that the PCL fibers retained their flexibility and length leading to the conclusion that MET encapsulated PCL fibers would be an ideal drug delivery system for periodontal diseases. Kim et al. also designed a drug delivery system in which PCL and polyethylene oxide (PEO) fibers were layered upon each other to form a drug reservoir mat. It was found that the rate of drug release was directly related to the thickness of the PCL fiber mesh layer. They also found that the protein used to test the DDS had not lost any biological activity, further demonstrating the viability of PCL as a possible drug delivery material [21].

Saeed et al. utilized PCL in the formation of PCL/Carbon nanotube composite fibers [22]. The carbon nanotubes were found to be well dispersed and oriented along the fiber axes. Castro et al. utilized PCL grafted nanotubes in developing a novel conductive polymer composite. This CNT/PCL conductive polymer composite showed promising results as a possible sensor for the identification of organic vapors [23].

Given the vast potential and successful application of PCL nanofibers it is imperative to develop and employ a method that can produce these nanofibers in greater yield. To the authors' knowledge, this article reports the first attempt to prepare PCL nanofibers using Forcespinning™ method. Therefore, the objective of this study was to determine the optimum processing

configurations and microstructure analysis of polycaprolactone fiber produced via Forcespinning™ technology. The effects of this method on the crystallinity of the polymer are analyzed using DSC and XRD.

2.2 Materials

All polymers and solvents were purchased from Aldrich (Milwaukee, USA) and were used without further purification. Polycaprolactone, with a number average molecular weight (M_n) of ~60,000, was dissolved in dichloromethane in concentrations of 16 and 18 wt%. In order to prevent solvent loss during mixing, the polymer solutions were sealed in scintillation vials for approximately 20 to 25 minutes and stirred using a magnetic stirrer.

2.3 Forcespinning™ Setup

Figure 1 shows a schematic diagram of the Forcespinning™ apparatus setup. The spinneret was equipped with 30 gauge ½ inch regular bevel needles (Beckett-Dickerson). Using a 10mL syringe either 2mL or 8mL of the polymer solution was injected into the spinneret. The selection of solution volume is a result of the particular spinneret size chosen.

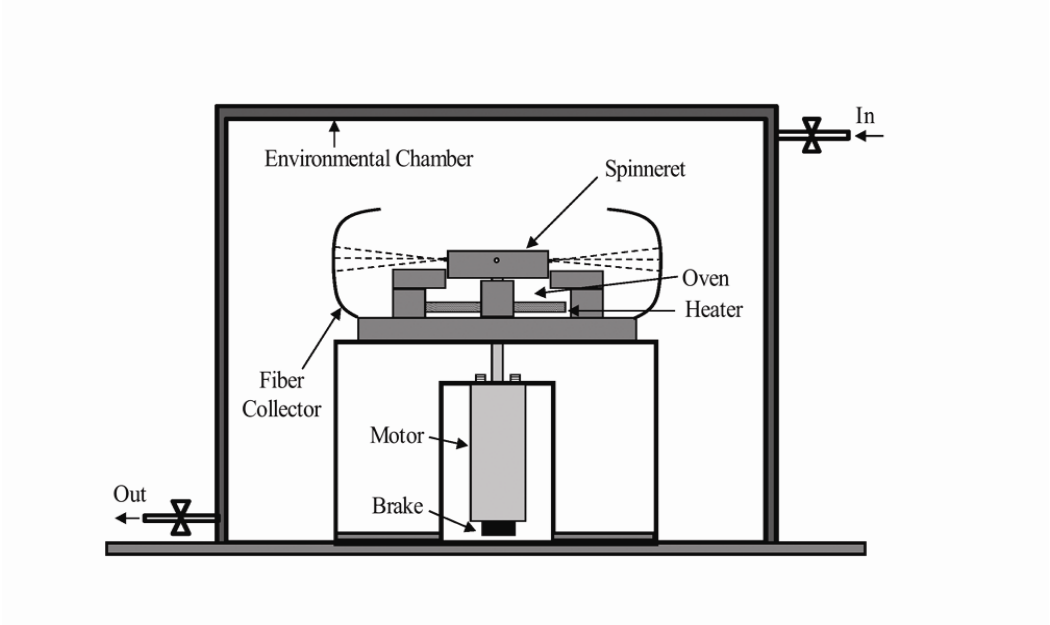

Figure 1: Schematic of Forcespinning™ setup.

The rotational speeds were varied from 3,000 RPM to 9,000 RPM. At 3000 RPM the solution was allowed to spin until depletion after approximately 30 seconds, where at 9000 RPM, it took approximately 10 seconds. A deep dish fiber collector with equally distanced vertical polytetrofluoroethylene (PTFE) pillars was used in order to collect fibers being elongated from the orifices of the spinneret. After collection the fibers were covered and stored under desiccation.

2.4 Fiber Morphology

The morphology of the collected PCL nanofibers (Figure 2) was analyzed using a BX51 optical microscope (Olympus, Tokyo, Japan) and an EVO LS10 scanning electron microscope (Carl Zeiss AG, Oberkochen, Germany) equipped with a SE detector. All samples were sputtered with gold-palladium using a Desk II sputter coater (Denton Vacuum, Moorestown, NJ) prior to SEM analysis.

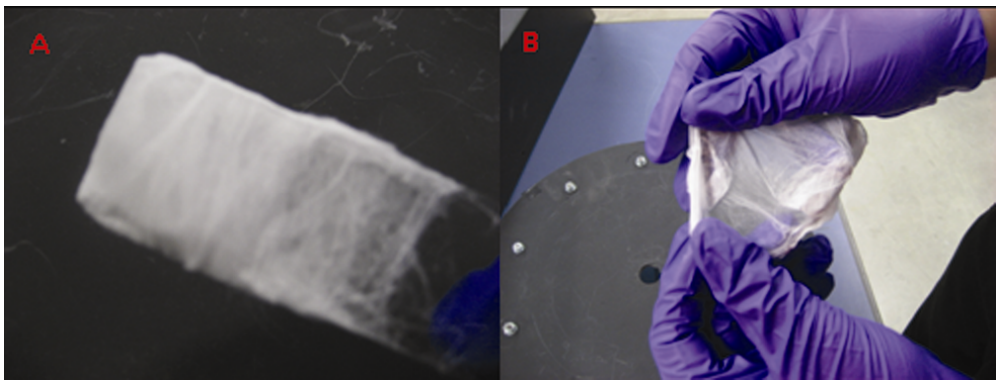

Figure 2: A) Fiber collection. B) PCL fiber mat.

2.5 Differential Scanning Calorimetry

Differential scanning calorimetery was conducted on all samples using a TA-Q Series 100 DSC (TA Instruments, Newcastle, DE). Samples weighing approximately 8-10 mg were sealed in aluminum hermetic pans and heated from 25°C to 215 °C at a rate of 5°C/min. All samples were heated under nitrogen purge with a balance purge flow rate of 40 mL/min.

2.6 X-Ray Diffraction

X-ray Diffraction studies were performed on all samples using an AXS D8 Discover Diffractometer (Bruker, Billerica, MA). XRD measurements were analyzed using Diffrac^{plus} EVA software (Bruker). The samples were scanned through a range of 15-70° 2θ angles using a 2D-detector.

2.7 Fiber Analysis

SEM micrographs of Forcespun fibers are shown in Figure 3. The fibers oriented in a random manner forming a three-dimensional mesh.

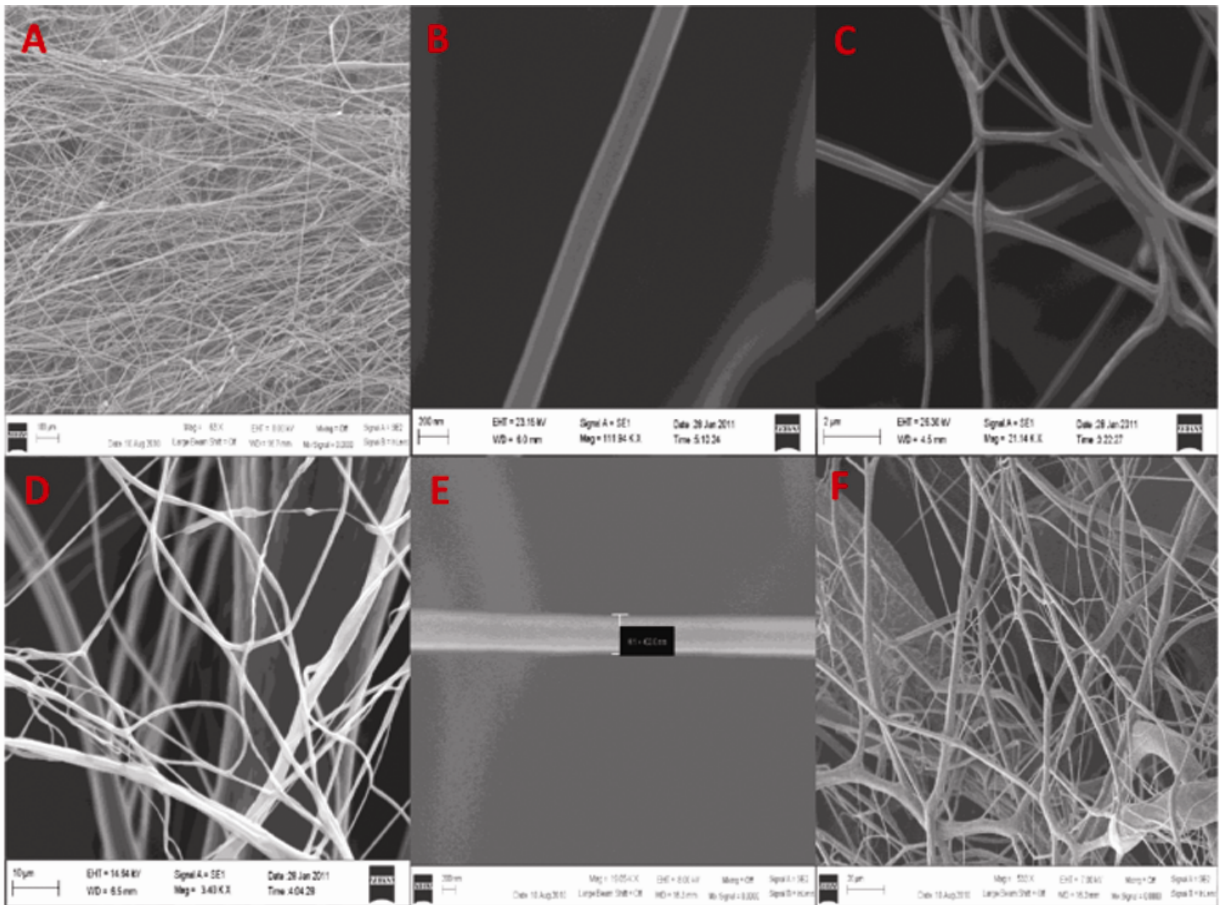

Figure 3: A) Fiber mesh 16% PCL-3000RPM. B) Single PCL fiber 16% spun at 3000 RPM. C) 16 % PCL fiber bundle spun at 3000RPM. D) Bundle of 16% PCL fibers spun at 6000 RPM. E) Single 16% PCL fiber spun at 9000 RPM. F) 16% PCL fiber bundle spun at 9000 RPM.

Although both 16wt% and 18wt% solutions were tested, the 16wt% solution was found to be optimal for sample preparation and handling. As can be seen in Table 1, the average fiber size for the 16wt% PCL fibers varied with spinneret speed. The smallest fiber average size was at 9000 RPM, though similar diameters were found at 3000 RPM. However it should be noted that the fibers analyzed at 9000 RPM had a lower standard deviation when compared to fibers formed at 3000 RPM.

Sample	Average Diameter (nm)	Standard Deviation (nm)
16%-3000RPM	264	± 125
16%-6000RPM	326	± 112
16%-9000RPM	220	± 98

Table 1: Fiber diameter of 16% PCL fibers spun at 3000 RPM, 6000 RPM, and 9000 RPM.

Also, the speed at which fibers were formed affected the beading of the fibrous mats. The SEM micrographs in Figure 4 show an overview of the fibrous mats and the difference in beading between them. It can be observed that the degree of beading formation has an inverse relationship with rotational spinneret speed. The fibers spun at 3000RPM had considerable beading while at faster rotational speeds beading decreased with fibers spun at 9000RPM having the least amount of beading.

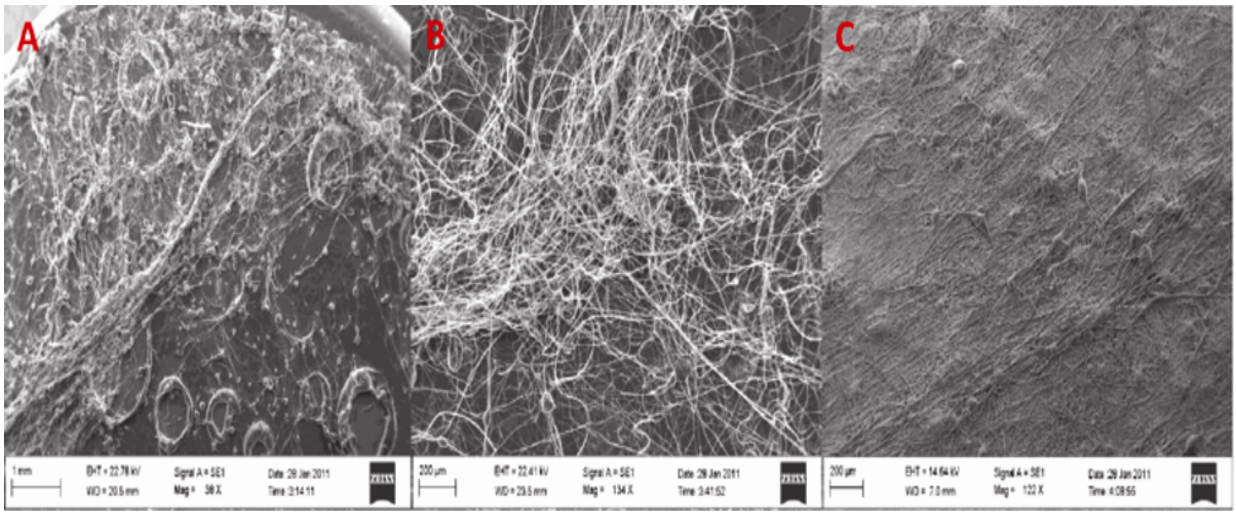

Figure 4: Effects of spinneret speed on beading of fiber mats. A) 3000 RPM B) 6000 RPM C) 9000 RPM

In addition, a study on the relationship between fiber diameters of collected samples after various collection times was conducted. Fiber samples of 16% PCL spun at 6000 RPM were collected after three 5 second intervals. It was found that as the time increased the average fiber diameter of the samples decreased and the standard deviation of the collected samples narrowed (Table 2). This indicates that after a critical time the average diameter of the collected fibers becomes more uniform (Figure 5).

Sample	Average Diameter (nm)	Standard Deviation (nm)
16%-5 Seconds	2105.2	±1004.3
16%-10 Seconds	1238.7	±895.5
16%-15 Seconds	508.7	±255.6
16%-30 Seconds	326.0	±112.0

Table 2: Fiber diameter of 16% PCL collected after spinning for 5sec, 10sec, 15sec, and 30sec.

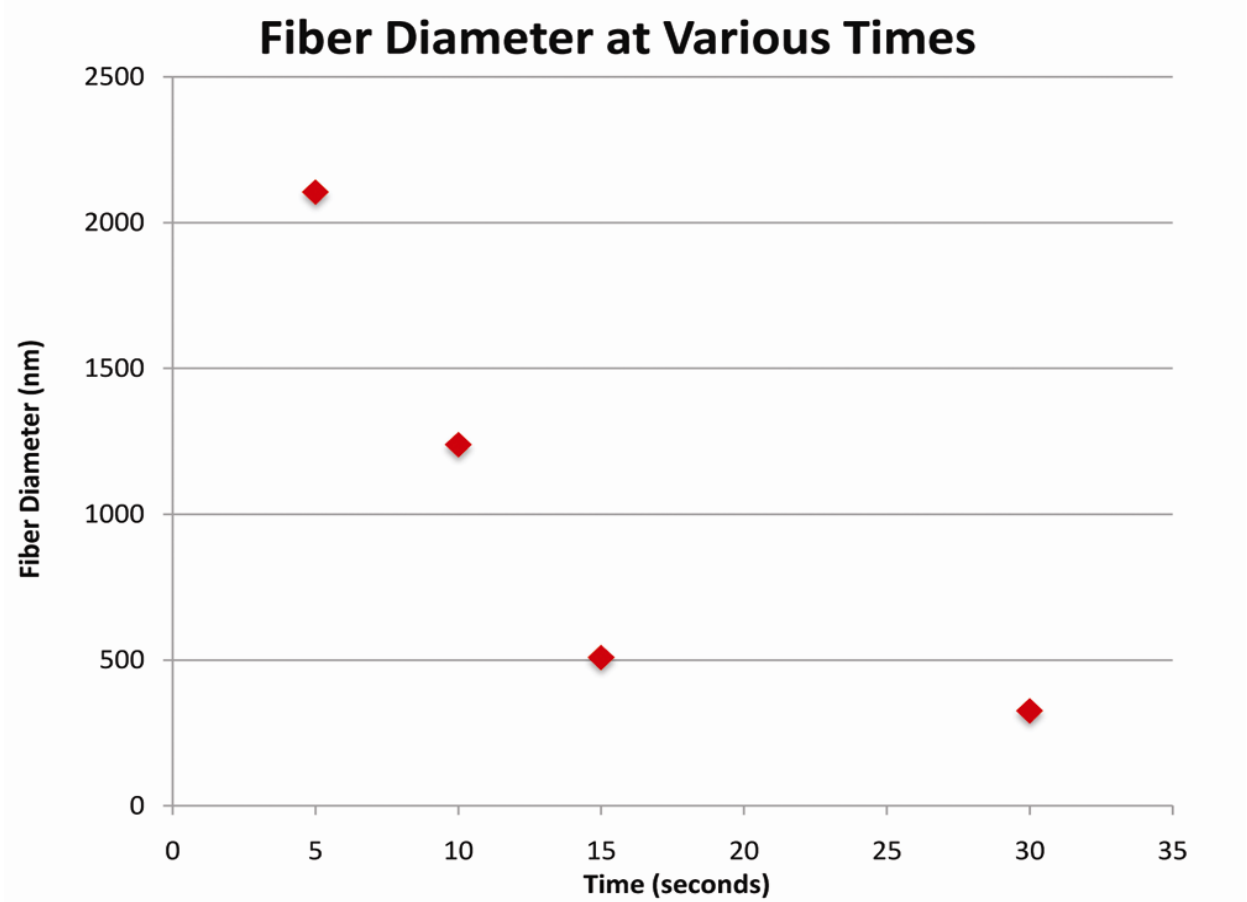

Figure 5: Graph of fiber diameter vs. time for the 16% 6000RPM PCL

This phenomenon is observed given that the fiber formation process is a combination of the imposed centrifugal force, the nozzle length and diameter, and the resultant aerodynamics forces that promote solvent evaporation and fiber elongation. In the first stage of the process, the polymer solution exits the nozzle in the form of a droplet that further elongates, given the viscoelastic properties of the material, slight swelling occurs at the tip of the nozzle which is overcame with time. If the system is stopped in the first stage, the fibers had not had time to overcome the elongation process nor has the solvent had time to evaporate. A complete theoretical and experimental study (including high speed camera analysis) regarding fiber formation is currently under preparation.

2.8 Crystallinity Studies

DSC data of both the bulk PCL and the 16wt% PCL nanofibers forcespun at speeds 3000RPM and 9000RPM were obtained and tabulated in Table 3. It is evident that the peak melting temperature (T_{mp}) of the nanofibers increased as well as the peak crystallization temperature (T_{cp}). However, the onset temperature of the melting endotherm (T_{op}) decreased. This lower onset temperature correlates with an extra peak apparent in the DSC melting endotherms of the fibers (Figure 6).

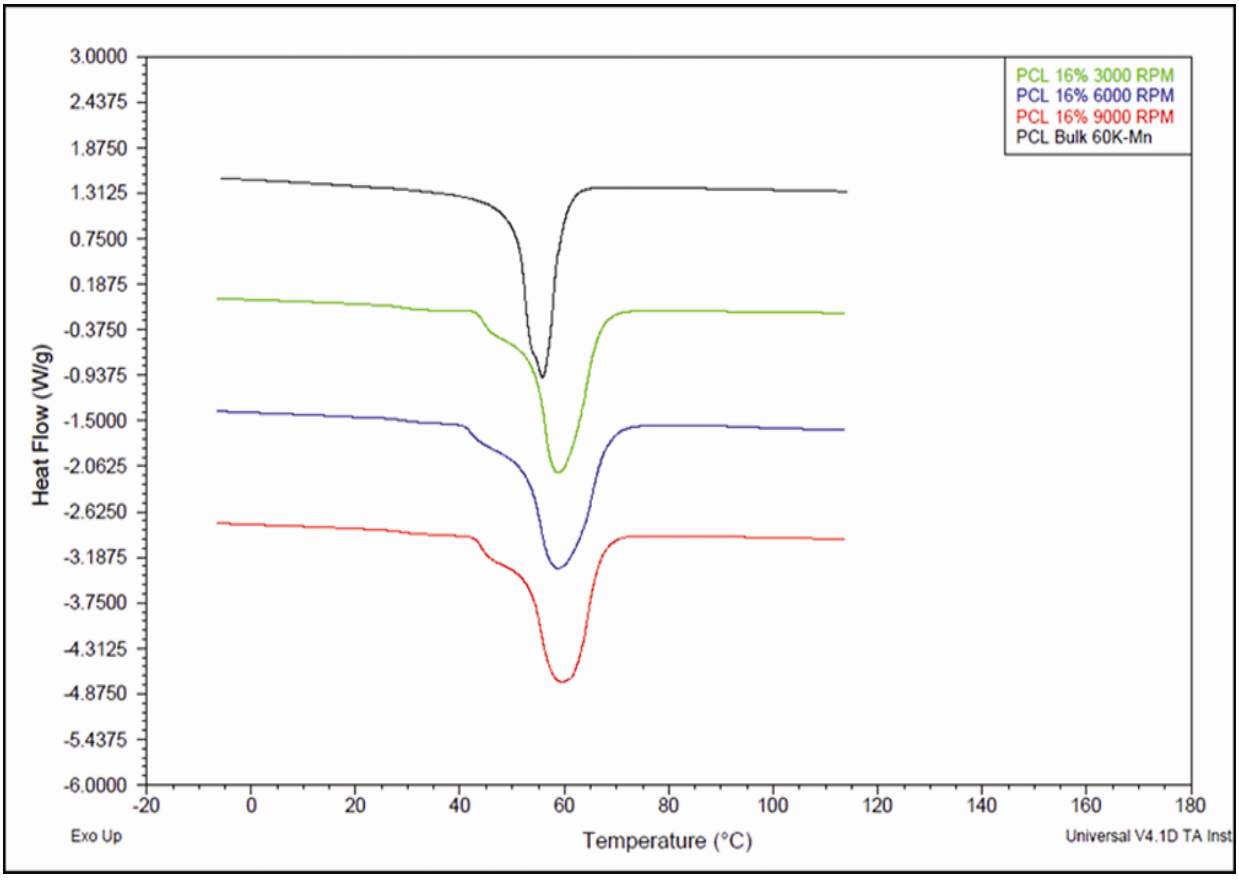

Figure 6: Melting endotherms of bulk PCL and 16% PCL forcespun fibers.

This decrease in onset temperature and the apparent second peak in the melting endotherm are attributed to the formation of an oriented mesophase resulting from incomplete crystallization due to rapid extensional flow. Figure 7 shows the endotherm peaks of the as-formed fibers and the second DSC cycle after deletion of thermal history.

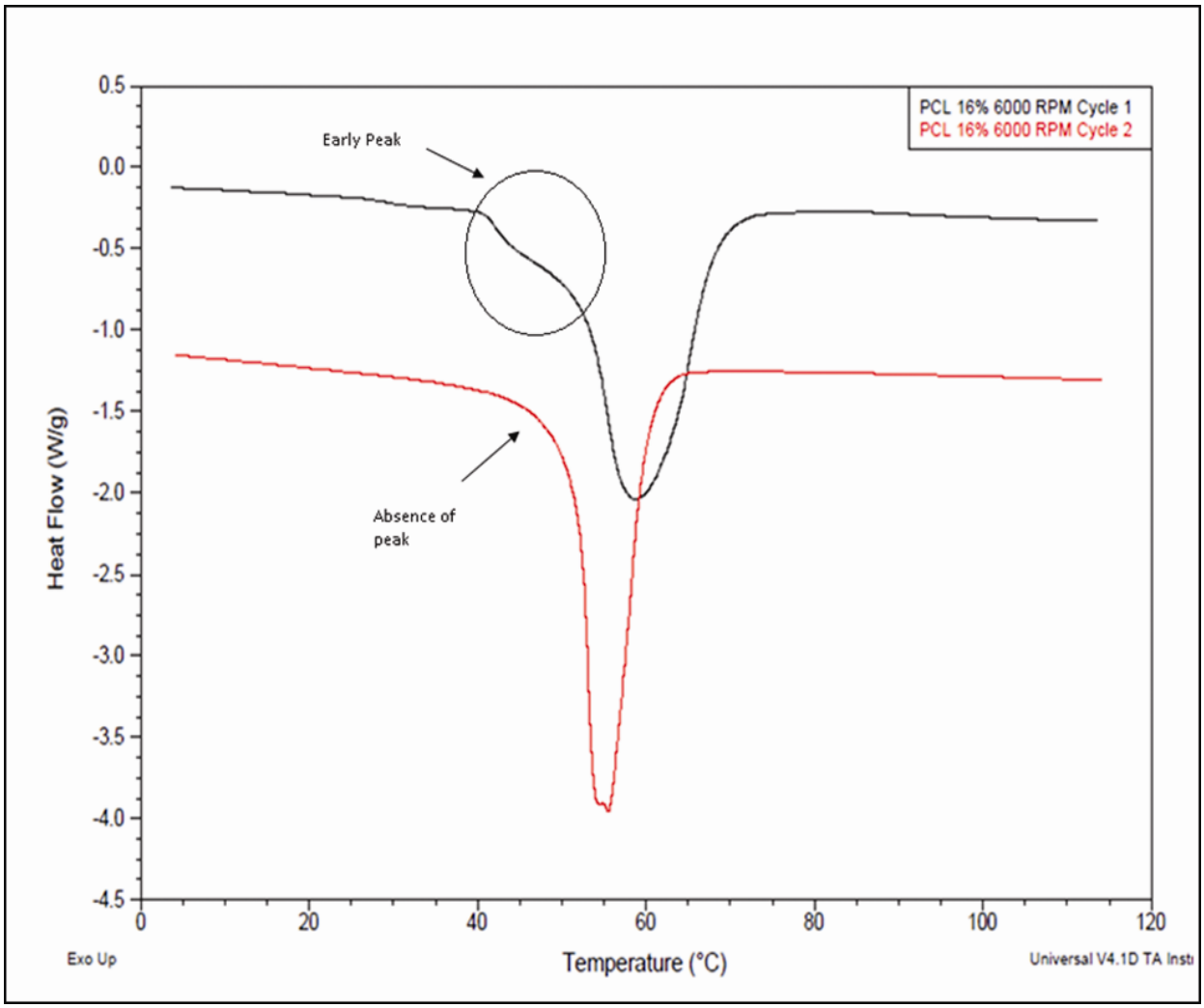

Figure 7: Melting endotherms of 16% PCL fiber showing absence of early peak after erasing of thermal history.

It can be seen that after erasing thermal history the original 16% fiber sample contains only one relatively sharp peak without the aligned mesophase. The crystallinity of each sample was calculated according to the equation:

Where:

= the enthalpy of fusion

= the enthalpy of cold crystallization

= the enthalpy of fusion of a 100% crystalline sample.

DSC data (Table 3) shows that the degree of crystallinity of the forcespun fibers decrease relative to the bulk sample. Moreover it can be observed that there is a decrease in the crystallinity of the 16% fibers with an increase in rotational speed.

Sample	Melting (T_m)			Crystallization (T_c)			% Crystallinity (χ_c)
	T_o	T_p	ΔH_m	T_o	T_p	ΔH_c	%
Bulk	51.5	55.81	110.5	30.40	22.58	78.00	23.2
16%-3000RPM	42.66	58.76	122.9	36.76	33.76	97.35	18.3
16%-9000RPM	43.36	59.61	120.0	34.90	28.84	95.85	17.3

Table 3: DSC data summary of bulk PCL and 16% forcespun fibers at different RPM.

As explained above, when fibers are rotated at higher speeds and longer times, the fiber diameter decreases, the polymer chains are further aligned given rise to the aligned mesophase with incomplete crystallization given fast elongation and solvent evaporation rate. Similar to electrospun fibers, the morphology and crystallinity of forcespun fibers seem to be highly dependent on both solvent evaporation rate and collector distance thus this decreased time frame of evaporation due to an increase in rotational speed ultimately restricts the extent to which crystallites are able to form in the collected fibers.

Figure 8 shows the X-Ray diffraction spectra for the bulk and PCL nanofibers. The intensity of the bulk peak is higher than that of the various fiber peaks.

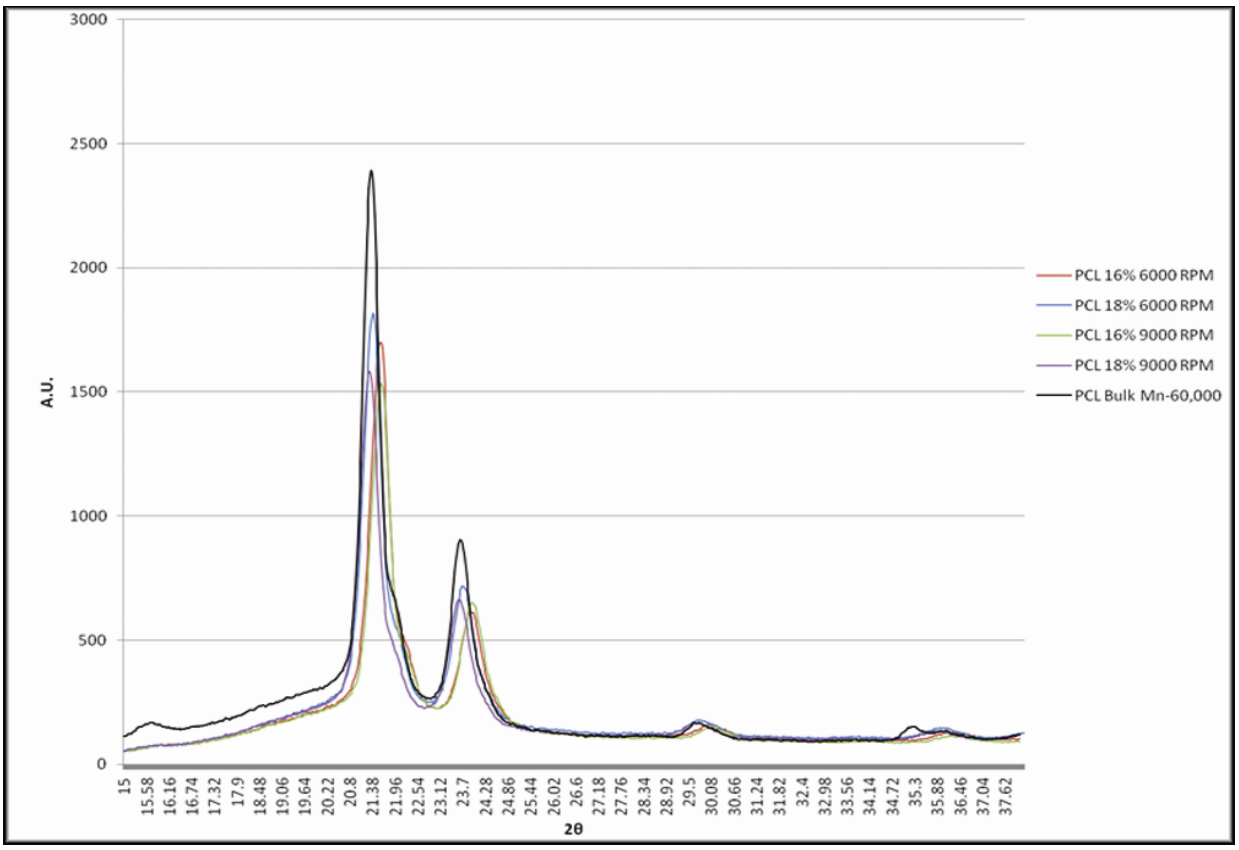

Figure 8: XRD spectra of 16% and 18% PCL fibers spun at 9000 RPM and 6000 RPM

Since crystallinity is a measure of the area of the peaks over the area of the whole, it can be determined that the production of polycaprolactone nanofibers via the Forcespinning™ method decreased crystallinity, which is consistent with the collected DSC data. Two intense 2θ peaks were observed at 2θ =21.5° and 2θ =23.9° these peaks coincide with previously observed 2θ peaks present in PCL fibers formed via electrospinning [24].

CHAPTER III

MICROCRYSTALLINE CELLULOSE/ROOM-TEMPERATRUE IONIC LIQUIDS

3.1 Introduction

Cellulose is one of the most abundant natural polymers found on earth [25]. Due to its composition, a linear polysaccharide with β-1-4 linked glucose molecules, cellulose presents excellent aqueous stability, biocompatibility and renewability. However, because of the strong equatorial hydroxyl groups present on glucose molecules, there are strong hydrogen bond interactions between the linear polymer chains (Figure 9).

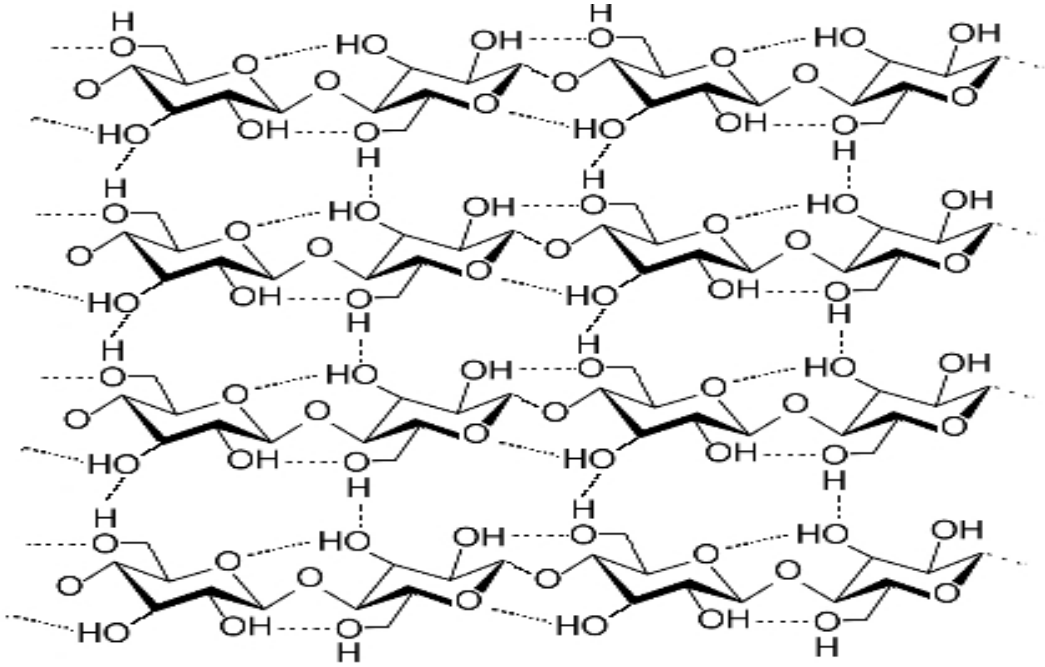

Figure 9: Hydrogen bonding between cellulose chains (*courtesy www.wikipedia.org*)

As a result, cellulose doesn't melt and it is soluble in very few organic solvents, thus processing bulk cellulose into fibers, especially in the micron and nanometer range, has presented a challenge. Cellulose derivatives such as cellulose acetate and cellulose hydroxyl propyl have been successfully processed into fibers using common organic solvents [25]; however the integrity of the cellulose polymer has been compromised due to the addition of ancillary functional groups. In addition, extra processing steps must be undertaken in order to recover pure cellulose fibers.

The dissolution of pure bulk cellulose and ultimately its processing into fibers has a rich history in the textile industry. The first large scale and successful production of cellulose fibers was the viscose method discovered in 1891 [26]. This process required cellulose to be converted to cellulose xanthate via treatment with an alkali agent and carbon disulphide and ultimately spun into fibers; however, many of the by-products associated with this process are toxic. A half decade later another method of cellulose production, termed the Lyocell method was discovered and proofed to be considerably more environmentally friendly. The Lyocell method consisted of dissolving native cellulose in an aqueous solution of the amine oxide, N-methylamine-N-oxide. However in recent years there has been a push to produce fibers on the micron and nanometer range, most notably via the electrospinning method. Kim et. al successfully electrospun pure cellulose from a solution of lithium chloride (LiCl) and N,N-dimethyl acetamide (DMAC) and Kulpinski was able to manufacture cellulose nanofibers from a solution of N-methylmorpholine-N-oxide (NMMO). Although these previously used solvents are promising for the production of cellulose nanofibers, they are volatile and relatively toxic. Recently, however, a new class of solvents termed room temperature ionic liquids (RTIL) has shown great promise for the dissolution of pure bulk cellulose [27], [28]. These novel solvents are regarded as a "green"

solvent because they have essentially zero vapor pressure, high thermal stability, and recyclability [29]. In addition, RTILs can easily be modified via a change in the cation or anion. Particularly with cellulose, the anion character plays a significant role in the solvating power of the ionic liquid. Thus, due to its biocompatibility and solvating powers RTILs have been recently used as base solutions for the electrospinning of cellulose fibers for a variety of purposes.

Linhardt et al. used the ionic liquid 1-ethyl-3-methylimidazolium benzoate to successfully dissolve and electrospin cellulose/heparin fibers with diameters in the micron range [30]. After cytocompatibility test, it was found that the fibers exhibited excellent cytocompatibility and the addition of the heparin increased the clotting kinetics of human whole blood. Similarly, Miao et al. successfully electrospun cellulose immobilized with the cell lytic enzyme, lysostaphin on it from a solution of 1-ethyl-3-methlimidazolium acetate for use as an antibacterial wound dressing [31]. The lysostaphin functionalized cellulose fibers showed antibacterial properties toward S. aureus bacteria and low toxicity of keratinocytes.

Akin to biomedical applications, studies on cellulose fibers processed from RTILs have been conducted in a variety of other applications as well. Linhardt et al. produced cellulose-MWCNT co-sheath fibers, using cellulose as the outer insulating sheath and the MWCNT as the inner conductive core [32]. Using cellulases, the cellulose sheath at the tips of the fiber were removed and a voltage applied. The maximum conductivity observed was 10.7S/m at a concentration of 45wt% MWCNT.

Given the potential of cellulose nanofibers and the recyclability of RTILs, it is important to discover and develop more novel methods for the higher yield production of unmodified cellulose from RTIL. In this study the authors utilize the robust technique of Forcespinning™

[6], [33], [34] to produce meshes of unmodified cellulose fibers processed from the room temperature ionic liquid 1-ethyl-1-methylimidazolium acetate. In addition a novel collection system is introduced in order to extract pure cellulose fibers. To the authors' knowledge this article reports the first attempt at the production of unmodified cellulose from RTIL using the Forcespinning™ technique. SEM studies were conducted to obtain the morphology and average diameter of the produced fibers. Furthermore, thermogravimetric analysis (TGA) and X-ray diffraction (XRD) were performed on both the bulk cellulose and the collected forcespun cellulose fibers. In addition, FTIR was utilized to confirm the absence of any chemical modification that might be induced with dissolution of cellulose in 1-ethyl-3-methylimidazolium acetate.

3.2 Materials

The ionic liquid 1-ethyl-3-methylimidazolium acetate was purchased from Aldrich (Milwaukee, USA) and used without further purification. Microcrystalline cellulose (Acros, AC38724-0010) and dimethyl sulfoxide were purchased from Fisher Scientific and used without further purification. Bulk cellulose was dissolved in 1-ethyl-3-methylimidazolium acetate in a concentration of 3% w/w. In order to facilitate dissolution of the cellulose polymer and ultimately production of fibers, dimethyl sulfoxide (5% w/w) was added to the solution. The solution was stirred using a magnetic stirrer for approximately 2 hours. Figure 4 shows a sample of the completely dissolved cellulose in 1-ethyl-3-methylimidazolium acetate and DMSO.

Figure 10: Dissolved microcrystalline cellulose in 1-ethyl-3-methylimidazolium acetate and dimethyl sulfoxide (DMSO).

3.3 Forcespinning™ Setup

Figure 1 shows a schematic diagram of the Forcespinning™ setup. The spinneret was equipped with 22 gauge regular bevel needles (Beckett-Dickerson). Using a 5mL syringe, approximately 2 mL of the cellulose-ionic liquid polymer solution was injected into the spinneret. The rotational speeds were varied between 4,500 RPM to 8,000 RPM. Ultimately, the solution was allowed to spin until depletion (approximately 30 seconds).

3.4 Collector Setup

Due to the lack of vapor pressure of the solvent, a unique collector system was constructed in order to collect the forcespun samples (Figure 11). A custom built poly(methyl methacrylate) structure with a lower and upper sink was affixed at the bottom. A third piece was

positioned diagonally between the lower and upper portions. A pump was used in order to create a self-contained recycling coagulation bath containing water. The forcespun fibers would land on the wet diagonal surface and ultimately collect in the lower sink. Upon collection, all fibers were washed approximately three times with additional DI water and once with ethanol.

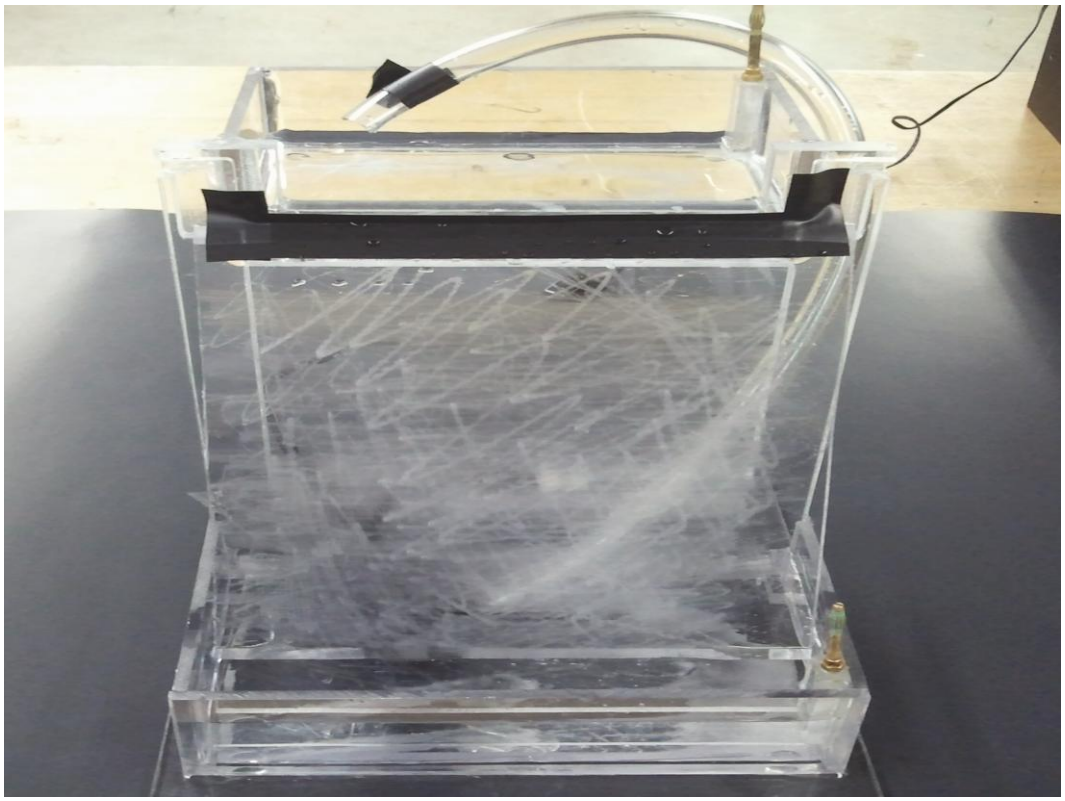

Figure 11: Collector system.

3.5 Fiber Morphology

Morphology studies of the bulk cellulose and forcespun cellulose fibers were conducted using a Sigma VP scanning electron microscope (Carl Zeiss AG, Oberkochen, Germany) equipped with a SE detector. Due to conducting SEM under VP mode, samples were not sputtered coated.

3.6 Fourier Transform Infrared Analysis (FTIR)

Fourier transform analysis was conducted on the bulk cellulose, regenerated cellulose film and collected forcespun cellulose fibers using a Thermo-Nicolet NEXUS 470 FTIR using a scan rate of 32 and a resolution of 16 cm^{-1}.

3.7 Thermogravimetric Analysis (TGA)

Thermal analysis was performed on the bulk and forcespun cellulose samples using a TA-Q Series 500 TGA (TA-Instruments, Newcastle, DE). Samples were heated from 25°C to 800 °C with a heat rate 5 °C/min. All samples were heated under nitrogen purge with a balance purge flow rate of 40 mL/min.

3.8 X-Ray Diffraction (XRD)

X-ray Diffraction studies were performed on both the bulk and forcespun samples using an AXS D8 Discover Diffractometer with a 2-D HISTAR General Area Diffraction Detection System (Bruker, Billerica, MA). XRD measurements were analyzed using Diffrac^{plus} EVA software (Bruker). The samples were scanned through a range of 10-45° 2θ angles using a 2D-detector with a 300 second exposure time.

3.9 Fiber Analysis and Characterization

Initially, fibers were collected in a water coagulation bath and rinsed multiple time using DI water and ethanol. The samples were then transferred to scintillation vials filled with DI water (Figure 12). As can be seen the fibers appear separated while suspended in water.

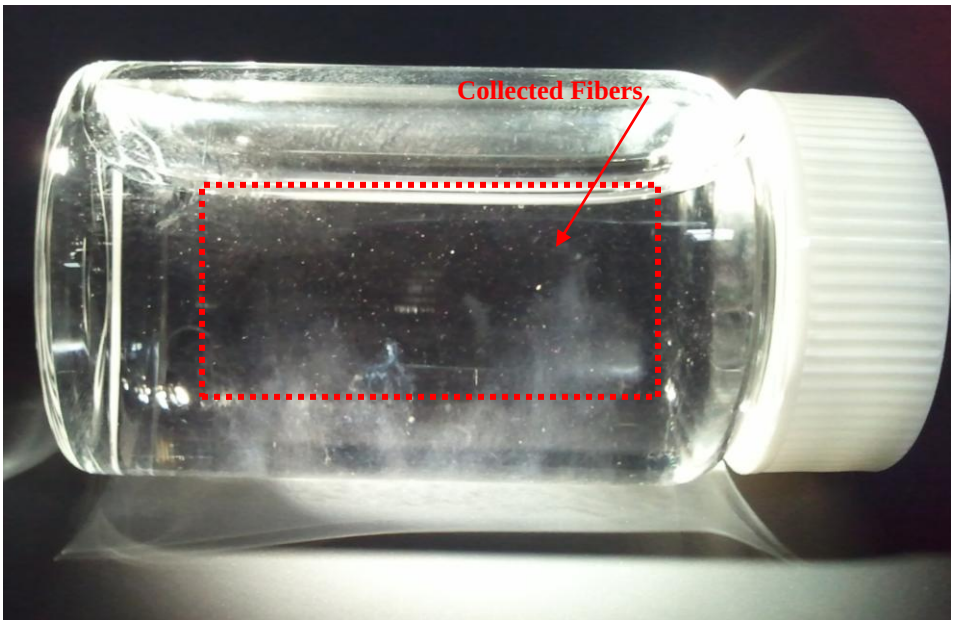

Figure 12: Fibers suspended in water

The apparent fiber separation while suspended in water is due in part to hydrogen bonding between the forcespun cellulose fibers and the water molecules. Interestingly enough, when the collected fibers are withdrawn from the scintillation vial, they tend to aggregate and appear as a jelly-like substance (Figure 13). The collected fiber were then placed on glass slides and subjected to heating at 80^{o}C for approximately 12 hours. Upon completion of heating the collected fiber appear to form a fibrous membrane as can be seen in Figure 14.

Figure 13: Collected fibers before drying.

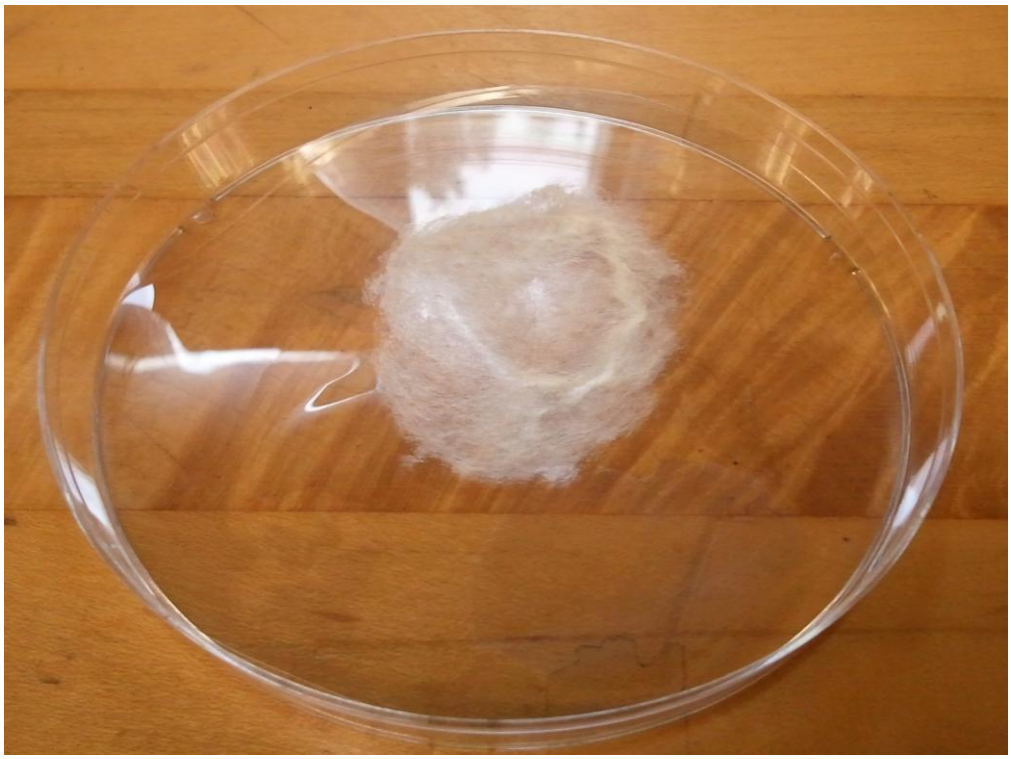

Figure 14: Collected fibers after drying.

The bulk and regenerated cellulose samples were used as reference samples. Many RPM speeds were tested, however the authors found that samples spun at 8000 RPM produced the best results and thus all data recorded is for samples spun at 8000 RPM. As can be seen in Figure 15 and Figure 16, the forcespun micro-crystalline cellulose samples exhibited a network of non-woven, continuous fibers.

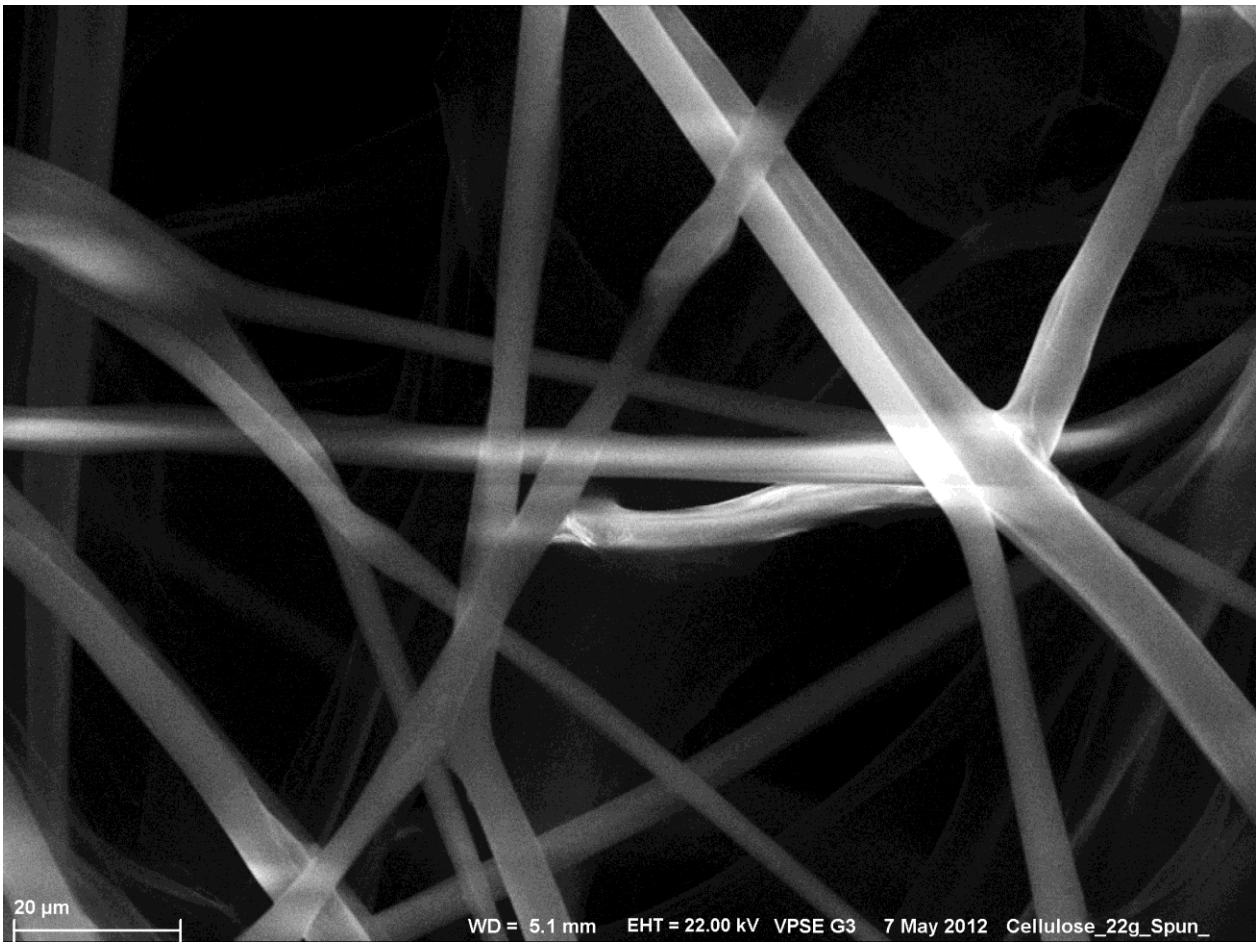

Figure 15: SEM micrograph of collected cellulose fibers.

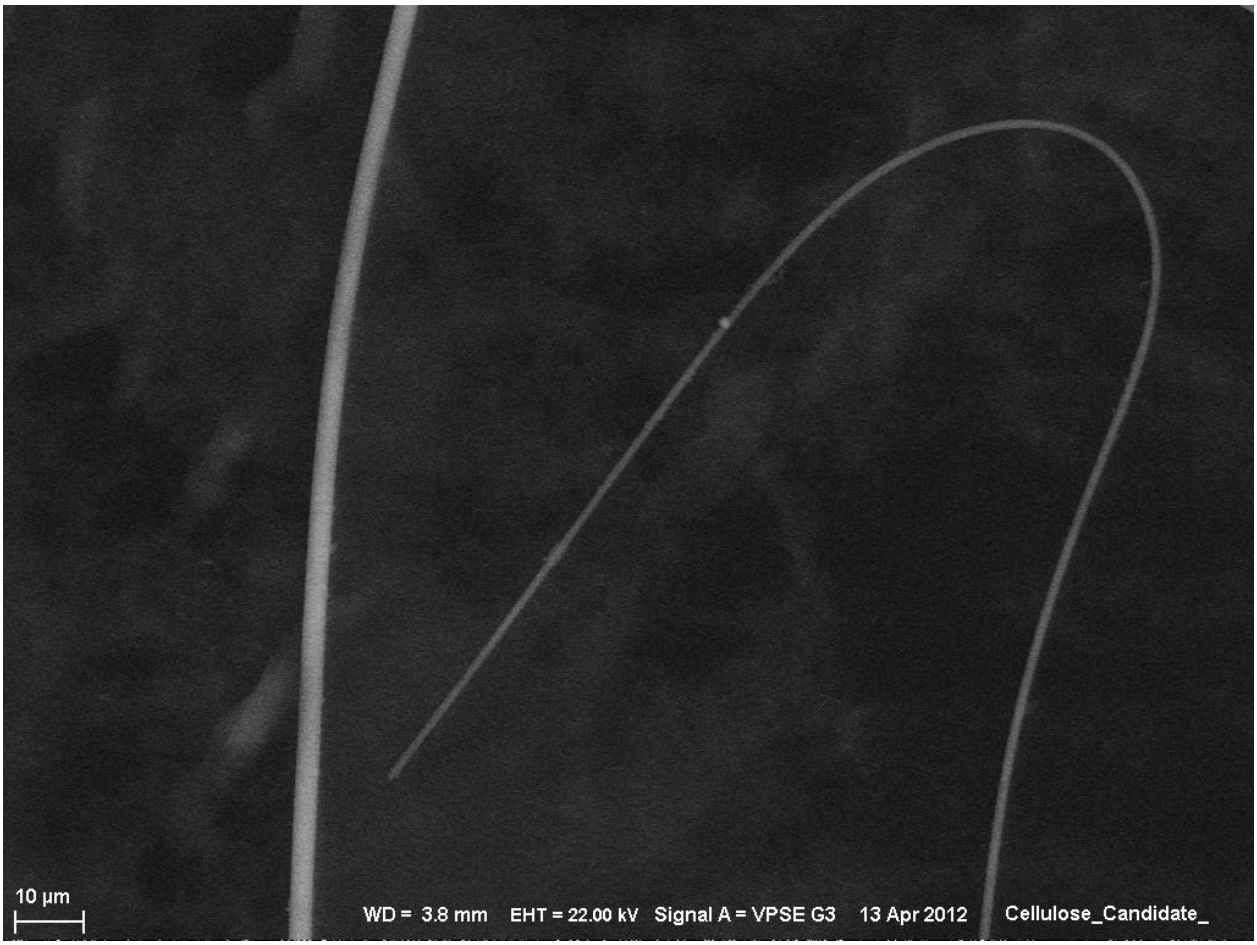

Figure 16: SEM micrograph of collected cellulose demonstrating the continuous nature of the fibers.

The diameters of the collected cellulose fibers ranged from nanometer sized to micron sized, with an average diameter of 4.665 microns and a standard deviation of 1.299 microns. However, statistical analysis (Figure 17) reveals that approximately 61% of the measured fibers had diameters between 3 to 5 microns. Additionally, there were a number of fibers with diameters in the sub-micron range (Figure 18)

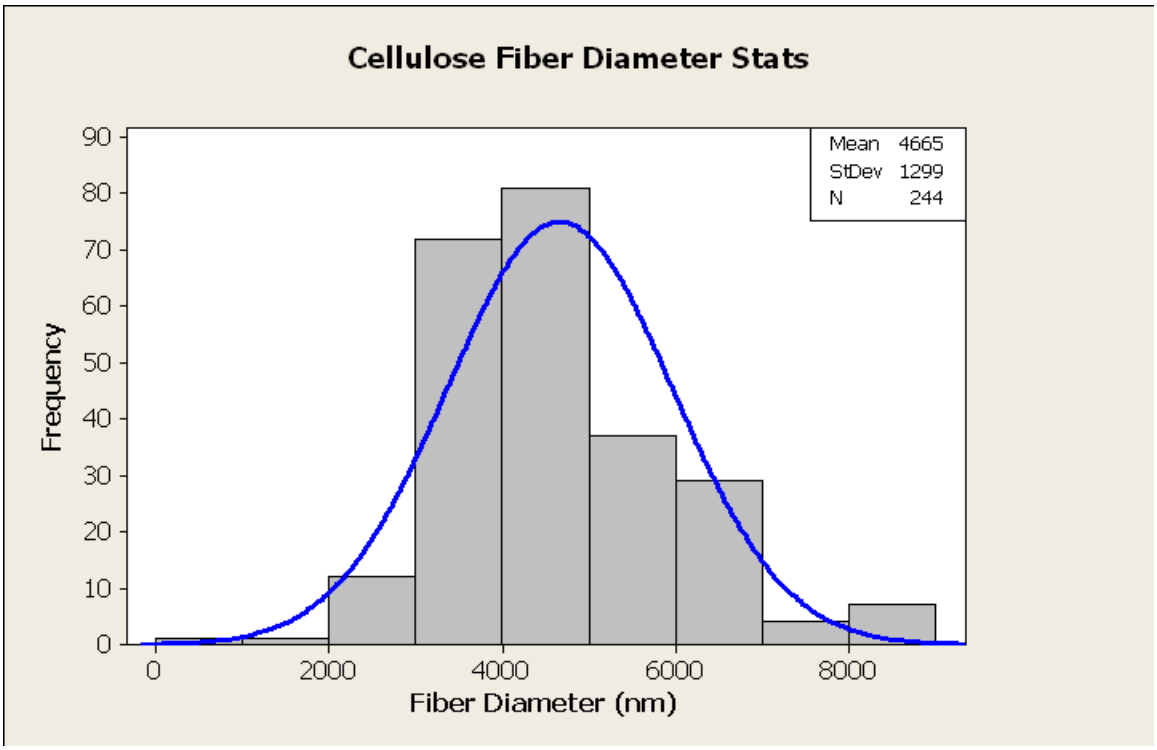

Figure 17: Histogram of collected fiber diameters.

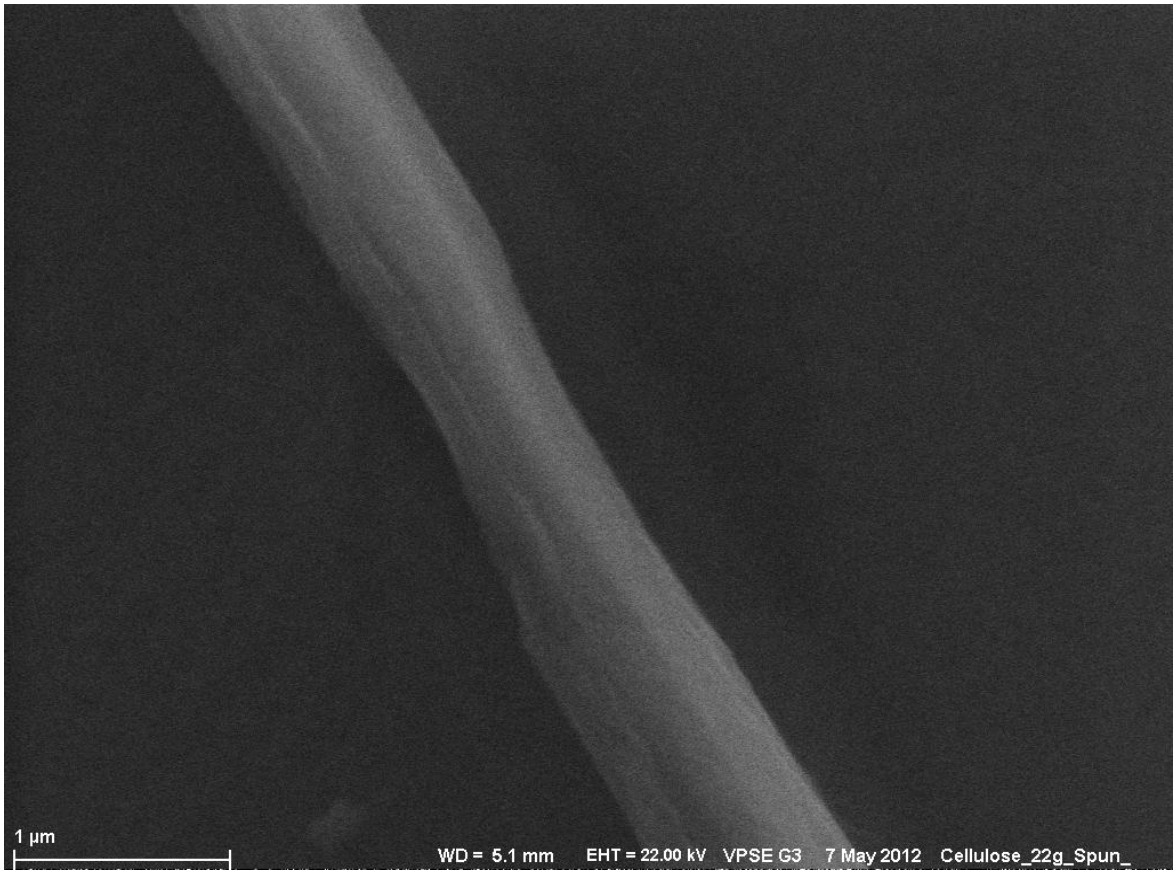

Figure 18: SEM micrograph of cellulose nanofiber

Furthermore, some portions of the collected fibrous mat showed signs of "webbing" between the fibers (Figure 19). This webbing may contribute to the macroscopic film like texture associated with the forcespun mats. Additionally, this is consistent with the similar "skin" like mats produced by *Xu et al.* using electrospinning [35]. The formation of webbing within the fibrous mats may be due in part to the fusion of the initial cellulose/[EMIM]Ac fibers before complete extraction of the RTIL in water.

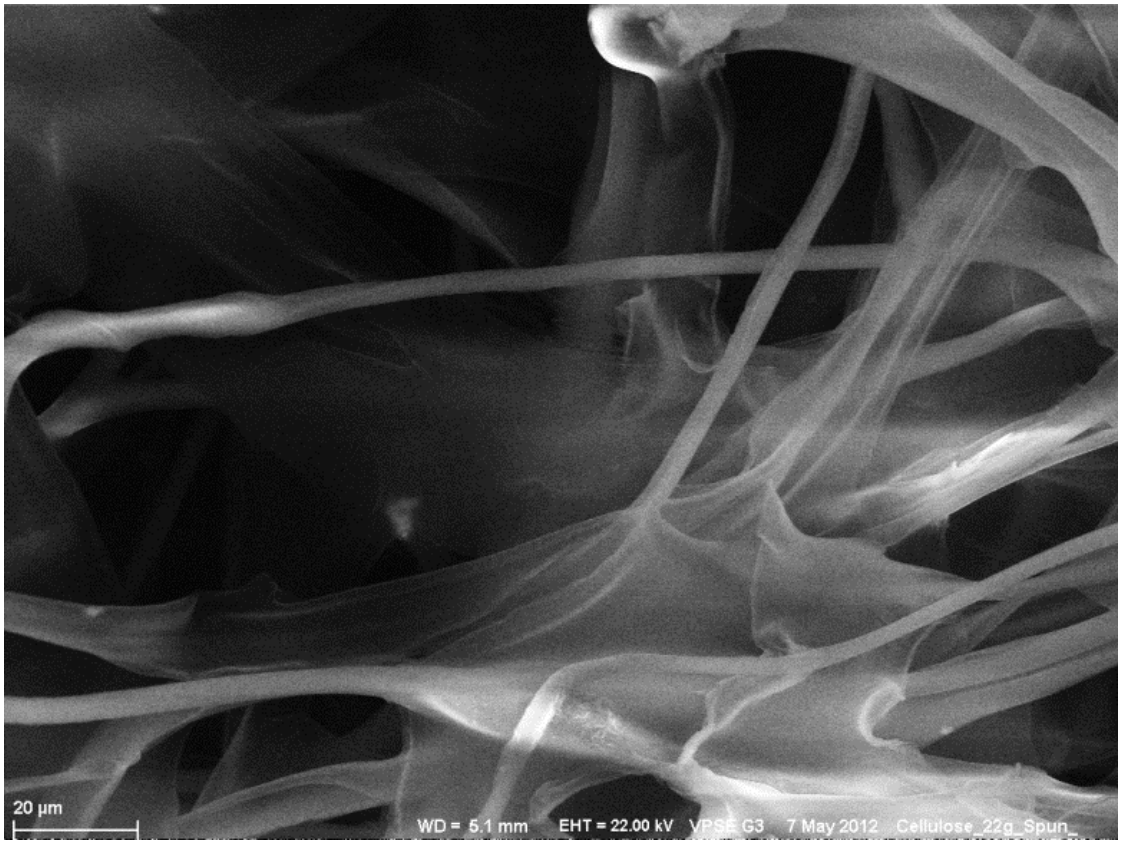

Figure 19: SEM micrograph showing "webbing" of cellulose fibers.

FTIR analysis was performed on the bulk cellulose and the forcespun cellulose fibers in order to determine if any derivativization of the bulk cellulose occurred during dissolution or forcespinning. As can be seen in the FTIR spectra (Figure 20), characteristic peaks at 1075 cm^{-1} and 1650 cm^{-1} are present in both the bulk cellulose and forcespun cellulose samples. It should be noted that the large OH peak at ~3450 cm^{-1} is due to the presences of water in the sample.

The collected forcespun fibers showed no indication of derivativization during either dissolution or the forcespinning process, additionally it can be seen that washing the collected fibers with water and ethanol successfully removed all ionic liquid from the forcespun samples.

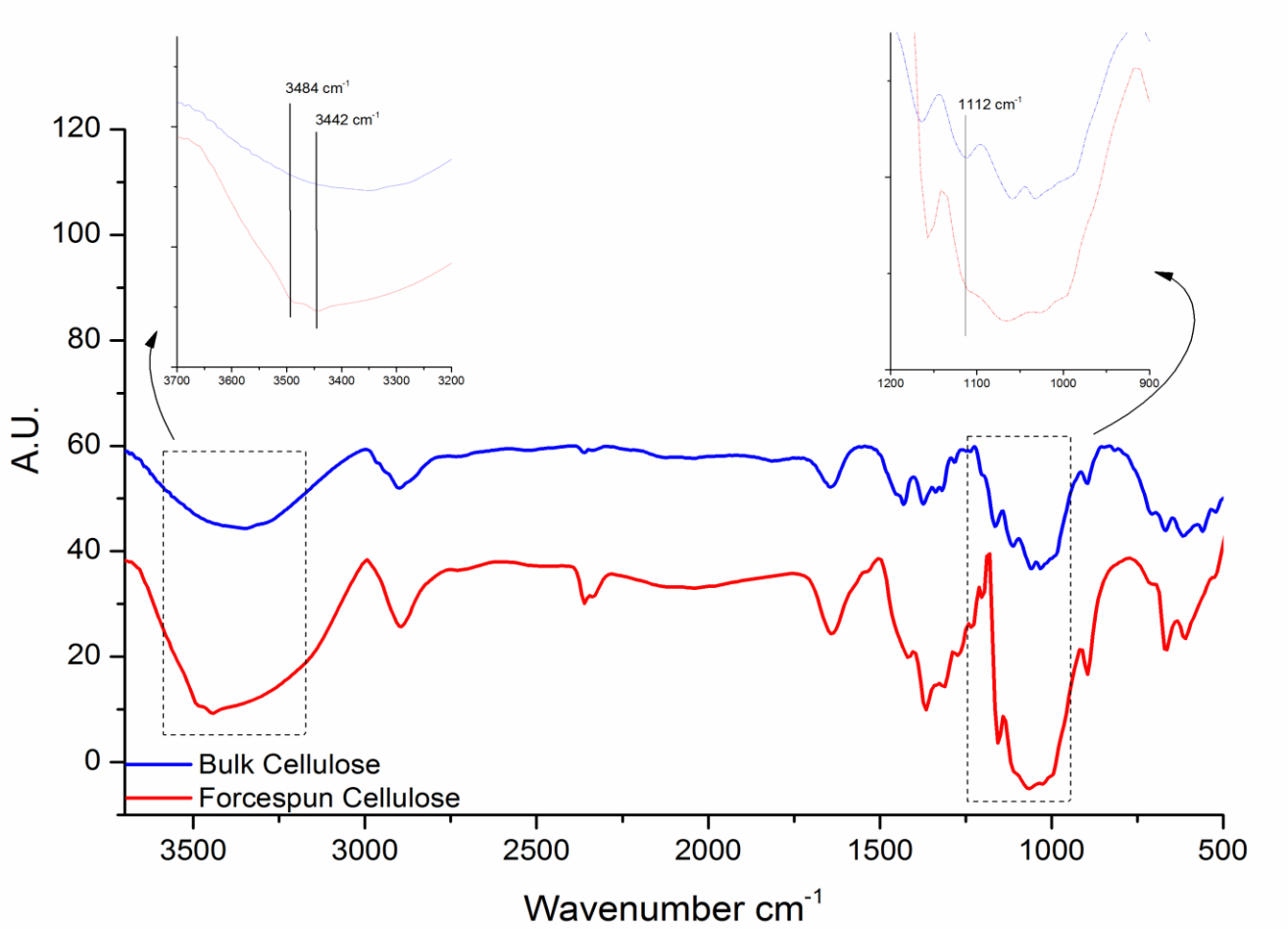

Figure 20: FTIR spectra of bulk cellulose and forcespun cellulose samples

Additionally, upon close analysis of the FTIR spectra it can be seen that there is a loss of the 1112 cm^{-1} peak in the forcespun cellulose as well the presence of two new peaks at 3484 cm^{-1} and 3442 cm^{-1}. These characteristic peaks indicate that the bulk cellulose is a Type-1 polymorph while the forcespun cellulose is a Type-2 polymorph [29].

Figure 21 below shows the X-ray diffraction spectra for the bulk cellulose sample and the collected forcespun cellulose. As can be seen, the bulk cellulose sample is a Type-I polymorph

with characteristic peaks at 2θ = 15.1°, 16.3°, 22.5°, 34.5° whereas, the forcespun cellulose is a Type-II polymorph with characteristic peaks at 2θ = 12.5° and 20.9°; this is consistent with the FTIR data above [36].

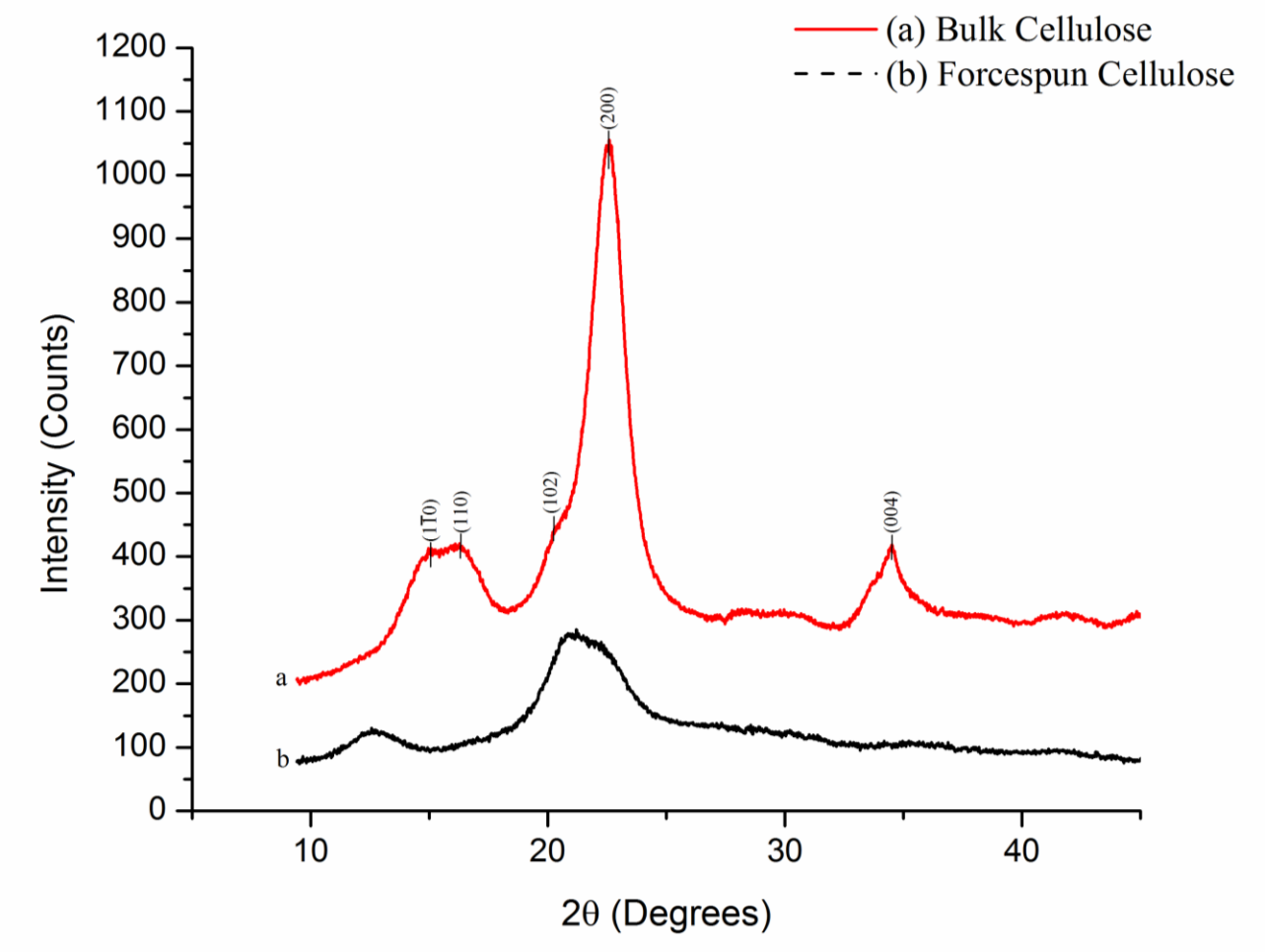

Figure 21: X-Ray diffraction peaks for (a) bulk cellulose and (b) forcespun cellulose

XRD analysis was also used in to calculate the relative crystalline index of both the bulk cellulose and the forcespun cellulose fibers. In order to calculate the crystallinity index, the peak height method (Seegal method) was employed. The formula for calculating the crystallinity index is given below.

Where, I_{200} is the maximum intensity of the 200 lattice diffraction (2θ=22.58) and I_{am} is the intensity of the lattice diffraction of the amorphous region (2θ=18.25°). It should be noted however that a slight modification of the above formula is needed in order to calculate the crystallinity index of the forcespun cellulose, i.e. a type II polymorph. Instead of using the maximum intensity of the 200 lattice diffraction, the maximum intensity at the 1 0 lattice diffraction is used instead, that is 2θ=16° for I_{am}. Table 4 summarizes the relative crystallinity values for the bulk cellulose and forcespun cellulose. Additionally the regenerated cellulose film Total Crystallinity Index (TCI) using FTIR was included as well. The data indicates that bulk cellulose as a higher relative degree of crystallinity than that of the forcespun cellulose; however it should be noted that the relative crystallinity of the regenerated forcespun fibers is near that of the bulk cellulose.

	Crystallinity Index (CrI) $\frac{I_{200} - I_{am}}{I_{200}} \times 100$	**Total Crystallinity Index(TCI)** $\frac{a_{1372\ cm^{-1}}}{a_{2900\ cm^{-1}}}$
Bulk Cellulose	.882	.597
Forcespun Cellulose Fibers	.819	.473
Regenerated Cellulose Films	----	.273

Table 4: Relative crystallinity of bulk cellulose and forcespun cellulose.

Lastly thermogravimetric analysis was performed on both the bulk cellulose and forcespun cellulose fibers (Figure 22). It was found that the forcespun fibers showed a lower onset degradation temperature, however the derivative peak temperature increased in the forcespun

sample. This increase in derivative peak temperature may be a result of the increased stability associated with cellulose Type-II polymorphs. Also, the initial mass loss of both the bulk and forcespun fibers can be attributed to water desorption.

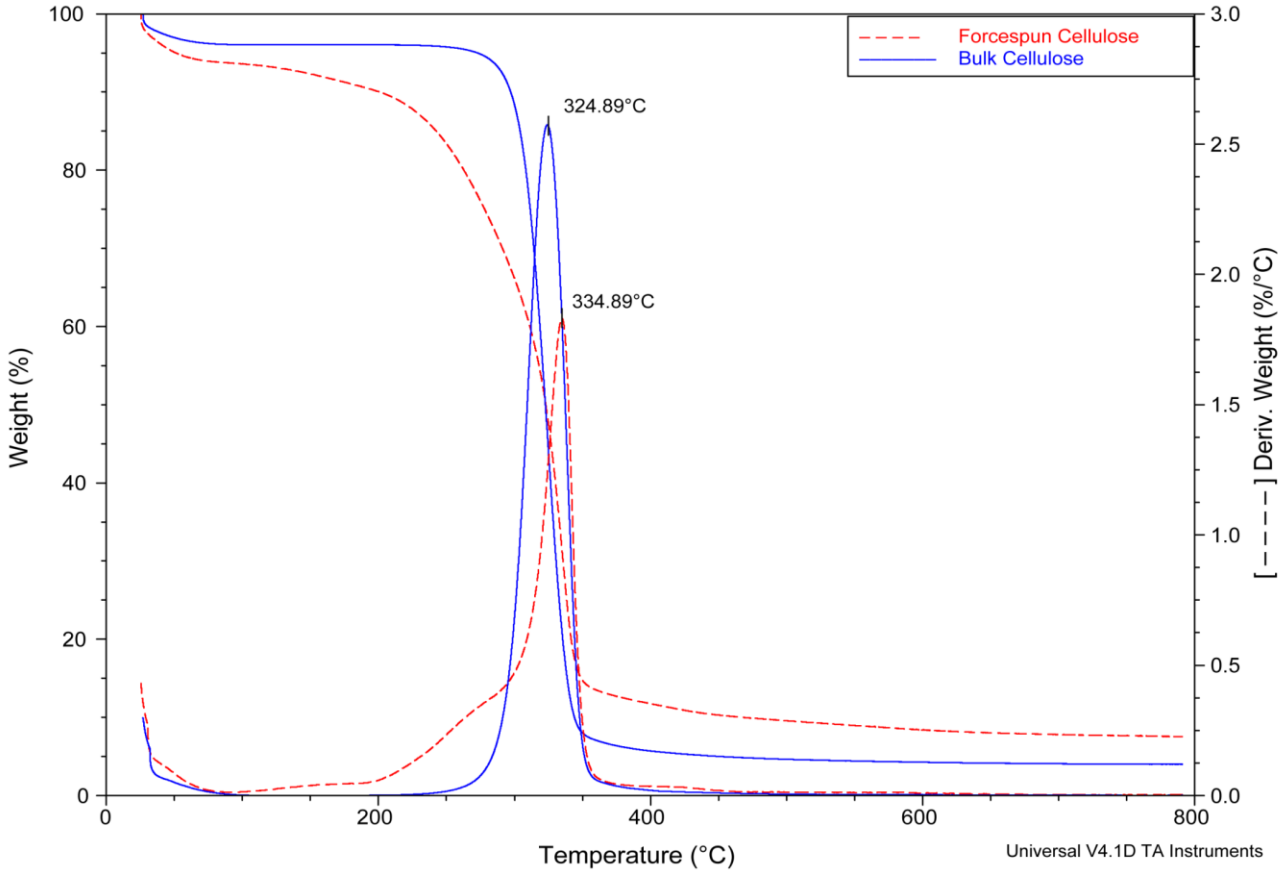

Figure 22: TGA thermogram for both bulk and forcespun cellulose.

CHAPTER IV

CONCLUSION

4.1 Polycaprolactone

Forcespinning™ Technology was utilized in order to produce polycaprolactone nanofibers. The degree of beading as well as the diameter size of the individual fibers is dependent on spinneret speed. It was found that fibers spun at 9000 RPM produced nearly bead-less mats as well as fibers with average diameters of 220nm. It was also found that the production of PCL fibers via Forcespinning™ technology induced a crystalline mesophase attributed to processing, which is not present in the bulk samples. It was observed that bulk PCL has a higher degree of crystallinity than PCL nanofibers and that fiber crystallinity was inversely proportional to rotational spinneret speeds. Forcespinning™ proves to be a successful method to fabricate long, continuous, and homogenous PCL nanofibers in high yield (at lease 1gr/min in the lab scale apparatus) where samples could be collected as nonwoven mats uniformly deposited on substrates or as free standing individual (continuous) fibers that can be aligned and spooled into yarns.

4.2 Microcrystalline Cellulose/Ionic Liquids

Similar to the first study, the Forcespinning method was employed to fabricate micro/nano-sized cellulose fibers from the ionic liquid 1-ethyl-3-methylimidazolium acetate. It was found that the Forcespinning method allowed for the high throughput production of

cellulose fibers with consistent diameters. Furthermore, the average diameter for the collected cellulose fibers ranged from approximately 0.6 microns to 8 microns, with an average diameter of 4.66 microns and a standard deviation of 1.3 microns. XRD analysis revealed that the forcespun cellulose fibers exhibited a different polymorph structure (Type-II) than that of the bulk cellulose (Type-I), this change in polymorph structure can be attributed to the breaking and reforming of intermolecular hydrogen bonding during the dissolution process of cellulose in the ionic liquid $[EMIM]^+Ac^-$ and its ultimate regeneration in the water coagulation bath. Additionally, both FTIR and XRD analysis revealed that the bulk cellulose has a higher relative crystallinity than that of the regenerated forcespun cellulose fibers. Lastly, thermograviemtric analysis showed a decrease in degradation onset temperature but an increase in derivative peak temperature in the forcespun fibers.

CHAPTER V

FUTURE WORK

In addition to the work presented above, the author would like to expand on these projects. Listed below are possible modifications or tests to the above experiments that the author is planning to possibly conduct.

5.1 Polycaprolactone

- Use higher rotational speeds (up to 20,000 RPM)
- Incorporate SWCNT or MWCNT into the polymer solution in order to obtain well-aligned nanotubes in the fibrous matrix.
- Cytocompatibility test.

5.2 Microcrystalline Cellulose/Ionic Liquids

- Use other presently available and ultimately cheaper ionic liquids in order to obtain fibers.
- Use supercritical CO_2 in place of RTIL as a neoteric green solvent for the production of cellulose fibers

REFERENCES

[1] H. Yoshimoto, Y. Shin, H. Terai and J. Vacanti, "A biodegradable nanofiber scaffold by electrospinning and its potential for bone tissue engineering," *Biomaterials,* vol. 24, pp. 2077-2081, 2002.

[2] Y. Ito, H. Hasuda, M. Kamitakahara, C. Ohtsuki, M. Tanihara, I. Kang and O. Kwon, "A composite of hydroxyapatite with electrospun biodegradable nanofibers as a tissue engineering materials," *Journal of Bioscience and Bioengineering,* vol. 100, pp. 43-49, 2005.

[3] T. Grafe and K. Graham, "Nanofiber webs from electrospinning," in *Nonwovens in Filtration-Fifth International Conference,* Stuttgart, 2003.

[4] Y. Karube and H. Kawakami, "Fabrication of well-aligned electrospun nanofibrous membrane on fluorinated polyamide," *Polymers for Advanced Technologies,* vol. 21, pp. 861-866, 2009.

[5] D. Li and Y. Xia, "Electrospinning of nanofibers:reinventing the wheel?," *Advanced Materials,* vol. 16, pp. 1151-1170, 2004.

[6] K. Sarkar, K. Lozano, S. Zambrano, M. Ramirez, E. de Hoyos and H. Vasquez, "Electrospinning to forcespinning™: a technological advancement," *Materials Today,* 2010.

[7] D. Paneva, F. Bougard, N. Manolova, P. Dubois and I. Rashkov, "Novel electrospun poly(ε-caprolactone)-based bicomponent nanofibers possessing surface enriched in tertiary amino groups," *European Polymer Journal,* vol. 44, pp. 566-578, 2008.

[8] A. Baji, Y. Mai, S. Wong, M. Abtahi and P. Chen, "Electrospinning of polymer nanofibers: effects on oriented morphology, structures and tensile properties," *Composite Science and Technology,* vol. 70, pp. 703-718, 2010.

[9] S. Ramakrishna, An Introduction to Electrospinning and Nanofibers Technology, Singapore: World Scientific Publishing Co., 2005.

[10] K. Lozano and K. Sarkar, "METHODS AND APPARATUSES FOR MAKING SUPERFINE FIBERS". United States Patent US20090280325 A1.

[11] K. Lee, H. Kim, M. Khil, Y. Ra and D. Lee, "Characterization of nano-structured poly(ε-caprolactone) nonwoven mats via electrospinning," *Polymer,* vol. 44, pp. 1287-1294, 2003.

[12] H. Cao, T. Liu and S. Chew, "The application of nanofibrous scaffolds in neural tissue engineering," *Advanced Drug Delivery Reviews,* vol. 61, pp. 1055-1064, 2009.

[13] L. Nair and C. Laurencin, "Biodegradable polymers as biomaterials," *Progress in Polymer Science,* vol. 32, pp. 762-798, 2007.

[14] D. Heath, P. Christian and M. Griffin, "Involvement of tissue transglutaminase in the stabilisation of biomaterial/tissue interfaces important in medical devices," *Biomaterials,* vol. 23, pp. 1519-1526, 2002.

[15] M. Woodruff and D. Hutmacher, "The return of a forgotten polymer-polycaprolactone in the 21st century," *Progress in Polymer Science,* vol. 35, pp. 1217-1256, 2010.

[16] H. Jeon, J. Kim, T. Kim, J. Kim, W. Yu and J. Youk, "Preparation of poly(ε-caprolactone)-based polyurethane nanofibers containing silver nanoparticles," *Applied Surface Science,* vol. 254, pp. 5886-5890, 2008.

[17] R. Nirmala, K. Nam, D. Park, B. Woo-il, R. Navamathavan and H. Kim, "Structural, thermal, mechanical, and bioactivity evaluation of silver-loaded bovine bone hydroxyapatite grafted poly(ε-caprolactone) nanofibers via electrospinning," *Surface and Coating Technology,* vol. 205, pp. 174-181, 2010.

[18] J. Choi, S. Lee, G. Christ, A. Atala and J. Yoo, "The influence of electrospun aligned poly(caprolactone)/collagen nanofiber meshes of self aligned skeletal muscle myotubes," *Biomaterials,* vol. 29, pp. 2899-2906, 2008.

[19] J. Porter, A. Henson and K. Popat, "Biodegrable poly(caprolactone) nanowires for bone tissue engineering applications," *Biomateials,* vol. 30, pp. 780-788, 2009.

[20] M. Zamani, M. Morshed, J. Varshosaz and M. Jannesari, "Controlled release of metronidazole benzoate from polycaprolactone electrospun nanofibers for periodontal diseases," *European Journal of Pharmaceutics and Biopharmaceutics,* vol. 75, pp. 179-185, 2010.

[21] G. Kim, H. Yoon and Y. Park, "Drug release from various thicknesses of layered mats consisting of electrospun polycaprolactone and polyethylene oxide micro/nanofibers," *Applied Physics A-Materials Science and Processing,* vol. 100, pp. 1197-1204, 2010.

[22] K. Saeed, S. Park, H. Lee, J. Baek and W. Huh, "Preparation of electrospun nanofibers of carbon nanotube/polycaprolactone nanocompoosite," *Polymer,* vol. 47, pp. 8019-8025, 2006.

[23] M. Castro, J. Lu, S. Bruzaud, B. Kumar and J. Feller, "Carbon nanotubes/polycaprolactone

composite vapour sensors," *Carbon,* vol. 47, pp. 1930-1942, 2009.

[24] S. Wong, A. Baji and S. Leng, "Effect of fiber diameter on tensile properties of electrospun poly(ε-caprolactone)," *Polymer,* vol. 49, pp. 4713-4722, 2008.

[25] M. Frey, "Electrospinning cellulose and cellulose derivatives," *Polymer Reviews,* vol. 48, pp. 378-391, 2008.

[26] D. Klemm, B. Heublein, H.-P. Fink and A. Bohn, "Cellulose: Fascinating Biopolymer and Sustainable Raw Material," *Angewandte Chemie International Edition,* vol. 44, pp. 3358-3393, 2005.

[27] R. Swatloski, S. Spear, J. Holbrey and R. Rogers, "Dissolution of cellulose with ionic liquids," *Journal of the American Chemical Society,* vol. 124, pp. 4974-4975, 2002.

[28] B. Kosan, C. Michels and F. Meister, "Dissolution and forming of cellulose with ionic liquids," *Cellulose,* vol. 15, pp. 59-66, 2008.

[29] M. Freire, A. R. Teles, R. Ferreira, L. D. Carlos, J. A. Lopes-da-Silva and J. A. Coutinho, "Electropsun nanosized cellulose fibers using ionic liquids at room temperature," *Green Chemistry,* vol. 13, pp. 3173-3180, 2011.

[30] G. Viswanathan, S. Murugesan, V. Pushparaj, O. Nalamasu, P. Ajayan and R. Linhardt, "Preparation of biopolymer fibers by electrospinning from room temperature ionic liquids," *Biomacromolecules,* vol. 7, pp. 415-418, 2006.

[31] J. Miao, R. Pangule, E. Paskaleva, E. Hwang, R. Kane, R. Linhardt and J. Dordick, "Lysostaphin-functionalized cellulose fibers with antistaphylococcal activity for wound healing applications," vol. 32, no. 36, 2011.

[32] M. Miyauchi, J. Miao, T. Simmons, J.-W. Lee, T. Doherty, J. Dordick and R. Linhardt, "Conductive Cable Fibers with Insulating Surface Prepared by Coaxial Electrospinning of Multiwalled Nanotubes and Cellulose," vol. 11, no. 9, 2010.

[33] Z. McEachin and K. Lozano, "Production and characterization of polycaprolactone nanofibers via forcespinning technology," *Journal of Applied Polymer Science,* p. DOI: 10.1002/app.36843, 2012.

[34] S. Padron, R. Patlan, J. Gutierrez, N. Santos, T. Eubanks and K. Lozano, "Production and characterization of hybrid BEH-PPV/PEO conjugated polymer nanofibers by forcespinning," *Journal of Applied Polymer Science,* p. DOI: 10.1002/app.36420, 2012.

[35] S. Xu, J. Zhang, A. He, J. Li, H. Zhang and C. Han, "Electrospinning of native cellulose from nonvolatile solvent system," *Polymer,* vol. 49, pp. 2911-2917, 2008.

[36] S. Quan, S. Kang and I.-J. Chin, "Characterization of cellulose fibers electrospun using

ionic liquid," *Cellulose,* vol. 17, pp. 223-230, 2010.

[37] K. Schenzel and S. Fischer, "NIR FT Raman spectroscopy-a rapid analytical tool for detecting the transofrmation of cellulose polymorphs," *Cellulose,* vol. 8, pp. 49-57, 2001.

[38] R. H. Newman, B. J.-C. Duchemin and M. P. Staiger, "Phase transformations in microcrystalline cellulose due to partial dissolution," *Cellulose,* vol. 14, pp. 311-320, 2007.

[39] H. Zhao, C. Jones, G. Baker, S. Xia, O. Olubajo and V. Person, "Regenerating cellulose from ionic liquids for an accelerated enzymatic hydrolysis," *Journal of Biotechnology,* vol. 139, pp. 47-54, 2009.

[40] S. Ha, L. Ngoc, G. An and Y.-M. Koo, "Microwave-assisted pretreatment of cellulose in ionic liquid for accelerated enzymatic hydrolysis," *Biosource Technology,* vol. 102, pp. 1214-1219, 2011.

[41] H.-P. Fink, P. Weigel, H. Purz and J. Ganster, "Structure formation of regenerated cellulose materials from NMMO-solutions," *Progress in Polymer Science,* vol. 26, pp. 1473-1524, 2001.

[42] L. Hardelin, J. Thunberg, E. Perzon, G. Westman, P. Walkenstrom and P. Gatenholm, "Electrospinning of cellulose nanofibers from ionic liquids: The effect of different cosolvents," *Journal of Applied Polymer Science,* vol. 125, pp. 1901-1909, 2012.

BIOGRAPHICAL SKETCH

Zachary McEachin

Zachary McEachin was born in Pensacola, Florida on January 15, 1987. After graduating from South Walton High School in 2005 he attend The Florida State University (FSU), earning his bachelor of science in Biochemistry in 2009. While at Florida State, he performed undergraduate research in the lab of Dr. Harold Kroto under the supervision of Dr. Prashant Jain and Dr. Steve Acquah. His undergraduate research focused on the synthesis of carbon based architectures and single crystal metal-organic frameworks (MOFs). Upon graduation, he moved to Mission, TX and enrolled in the master's program in mechanical engineering at the University of Texas-Pan American. During his two years at UTPA, Zachary worked as a graduate research assistant in the lab of Dr. Karen Lozano. In April 2012, Zachary and Dr. Lozano published a paper in the *Journal of Applied Polymer Science* entitled Production and Characterization of Polycaprolactone Nanofibers via Forcespinning Technology. In July 2012, Zachary successfully completed his Masters of Science in Mechanical Engineering. Currently, Zachary his pursuing his PhD at the Georgia Institute of Technology/Emory University/ Peking University's joint program in biomedical engineering.